

Properties of sound-induced modulated structures in liquid crystals

D. I. Anikeev and O. A. Kapustina

Academician N. N. Andreev Acoustics Institute, Russian Academy of Sciences, 117036 Moscow, Russia

(Submitted 26 April 1996)

Zh. Éksp. Teor. Fiz. **110**, 1328–1338 (October 1996)

The effect of the angle ψ_0 between the director \mathbf{n}_0 and the velocity vector \mathbf{v} of a sound-induced oscillatory hydrodynamic flow in a planar capillary on the orientational instability of a planar layer of a nematic liquid crystal (NLC) is investigated. The conditions under which striped structures of different scale and incommensurate structures appear are determined and discussed. The threshold characteristics of the instability are determined and a classification criterion for the striped structures is substantiated experimentally. It is shown that besides the previously observed structures with period $\Lambda \sim d$ (Guyon–Pieranski roll instability, $\psi_0 = 90^\circ$), there exist structures with period $\Lambda < d$. It is also shown that a generalized theoretical model, based on the standard ideas of nematodynamics and employing a system of linearized Leslie–Ericksen–Parodi equations, describes completely satisfactorily the threshold characteristics of the instability. This confirms the theoretical picture. The mechanism of the transformation of the striped structures into incommensurate structures is examined. It is shown that this transformation is associated with the interaction of shear and longitudinal oscillations in the NLC via the oscillatory Couette and Poiseuille flow fields. © 1996 American Institute of Physics. [S1063-7761(96)01310-8]

1. INTRODUCTION AND FORMULATION OF THE PROBLEM

The action of acoustic oscillations on a two-dimensionally oriented layer of a nematic liquid crystal (NLC) under certain conditions changes the ordering of the molecules, the change being manifested in the formation of spatially modulated structures of different scales.¹ At present, there exist two approaches for analyzing such structures: nonequilibrium hydrodynamics and Leslie–Ericksen hydrodynamics.² The first approach was recently substantiated in a study of orientational phenomena at ultrasonic frequencies, for which the thickness d of the NLC layer and the wavelengths λ_v of the viscous waves and the wavelengths λ of the elastic waves satisfy $\lambda_v(\omega) \ll d \ll \lambda(\omega)$.³ The mechanism leading to the formation of modulated structures induced in oscillatory flows of a nematic liquid by the action of sound at frequencies satisfying the condition $\lambda_v(\omega) \gg d$ has been interpreted on the basis of the second approach.^{4–7} However, this effect has been studied thus far only in the particular case when the angle ψ_0 between the director \mathbf{n}_0 and the flow velocity equals 90° and the well-known Guyon–Pieranski instability arises.^{4–6} Very limited data are also available about structures formed in planar Couette flow with the director oriented parallel to the flow velocity vector \mathbf{V} .⁷

In the present paper we study the appearance of modulated structures in a NLC layer, located between the plates of a flat capillary, in an oscillatory Couette flow for arbitrary values of the angle ψ_0 between the flow velocity and the director. The experimental data on the formation conditions and properties of the structures are interpreted on the basis of a generalized theoretical model,⁸ which was developed using the same standard approach as in Refs. 4–7, Leslie–Ericksen hydrodynamics.

This model examines the following physical situation: a NLC is located between the planes $z=d$ and $z=0$ (Fig. 1);

the ends of the layer are open; the external action is set by the oscillations of one of the planes in the direction of the y axis according to the law $\xi_y(t) = \xi_{0y} \sin \omega t$, where $\xi_y(t)$ and ξ_{0y} are, respectively, the displacement and amplitude of the displacements and we write $\omega = 2\pi f$, where f is the frequency of the oscillations; the velocity profile of the oscillatory flow induced by these oscillations is $V_x = V_z = 0$ and $V_y = S(t)z$, where $S(t)$ is the velocity gradient; the director \mathbf{n}_0 lies in the plane of the layer and makes an angle ψ_0 with the flow direction (y axis).

2. EXPERIMENT

The experimental NLC—a eutectic mixture of MBBA and EBBA—filled a flat capillary formed by glass plates. The thickness of the layer was varied in the experiments in the range 10–150 μm . The observations of the orientational state of the layer were performed in transmitted polarized light using the standard schemes.¹ To produce the initial planar orientation of the ensemble of molecules, the inner surfaces of the plates were coated with polyvinyl alcohol and then polished in a definite direction.

Oscillations of one of the plates of the capillary in the direction of the y axis in the xy plane were produced by an electrodynamic exciter, powered by an acoustic-frequency generator whose frequency was varied in the range 1–20 Hz. The apparatus made it possible to rotate the capillaries relative to the “axis” of the oscillations of the exciter, so that the angle between the direction of this axis, the flow velocity vector and the director \mathbf{n}_0 can be varied from 0 to 90° . The amplitude ξ_{0y} of the oscillations of the mobile plate was measured by observing under a microscope the displacement of a reference line applied on the surface of the plate.

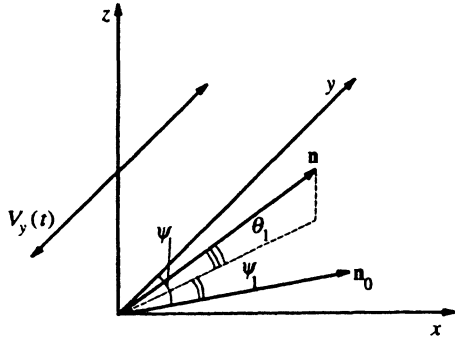


FIG. 1. For analyzing the threshold characteristics of the orientational instability in NLC. a—Geometry of the problem; the velocity profile of oscillatory planar Couette flow is $V_{0x}=V_{0z}=0$, $V_{0y}=S(t)z$, $S(t)$ is the velocity gradient; d —thickness of the NLC layer, \mathbf{n} and \mathbf{n}_0 are the instantaneous and initial positions of the director; θ_1 is the angle between the tilted position of the director \mathbf{n} and the plane of the layer xy ; $\psi_1 = \psi - \psi_0$, ψ is the angle between the projection of the director \mathbf{n} on the xy plane and the y axis; ψ_0 is the angle between the flow velocity vector and \mathbf{n}_0 .

3. EXPERIMENTAL RESULTS AND DISCUSSION

There exists a threshold amplitude $\varepsilon_{0 \min}$ of the oscillations at which the nematic-liquid flow oscillating along the y axis produces a nonuniform distribution of the director that is periodic along the x axis and that gives rise to a corresponding change in the index of refraction for light whose polarization vector \mathbf{E} is directed along the x axis. The system of cylindrical lenses formed in this manner focuses the transmitted light beam into bright lines oriented parallel to the y axis. The typical optical pattern of the distortions which is observed in polarized light ($\mathbf{E} \parallel \mathbf{x}$) is displayed in Fig. 2a ($d=60 \mu\text{m}$, $\psi_0=90^\circ$, $f=5 \text{ Hz}$). This is a system of stripes oriented parallel to the y axis with period $\Lambda = 2\pi/q$ along the x axis. In our experiments Λ was determined according to the position of the illumination maxima in the diffraction pattern produced by the optical phase grating;¹⁾ here, q is the wavenumber of the structure which is periodic along the x axis.

A typical plot of the wave number versus the displacement amplitude is displayed in Fig. 3; here, $d=35 \mu\text{m}$, $\psi_0=90^\circ$, $f=20 \text{ Hz}$. One can see that near threshold the wave number is smaller than above threshold and it becomes constant at $\psi_{0y} \approx 1.1\psi_{0y, \min}$. The modulated (striped) structures exist for values of ξ_{0y} in the range $\xi_{0y, \min} \leq \xi_{0y} \leq \xi_{0y1}$, where ξ_{0y1} is the displacement amplitude corresponding to a transition of the flow of the nematic liquid into an orientational turbulence regime.⁹

Data on the effect of the angle ψ_0 on the periodicity of the striped structure are presented in Fig. 4. Here, the wave numbers q are normalized to the values of q_0 corresponding to the distortion pattern with $\psi_0=90^\circ$ and $d=35 \mu\text{m}$. The frequency f of the oscillations is a parameter and assumes values of 2, 5, 15, and 20 Hz (symbols 1–4). As one can see, the wave number of the resulting structure depends on the angle ψ_0 , and as this angle decreases, an instability with smaller values of q develops. For the experimental NLC, the largest changes in q occur in the range of angles 40° – 50° . The values of q_0 to which the instantaneous values of q are

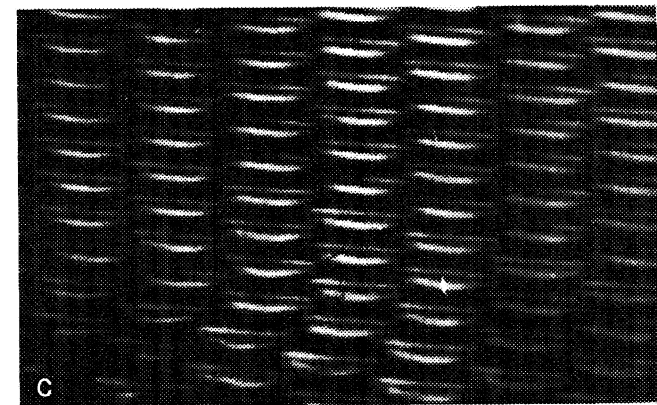
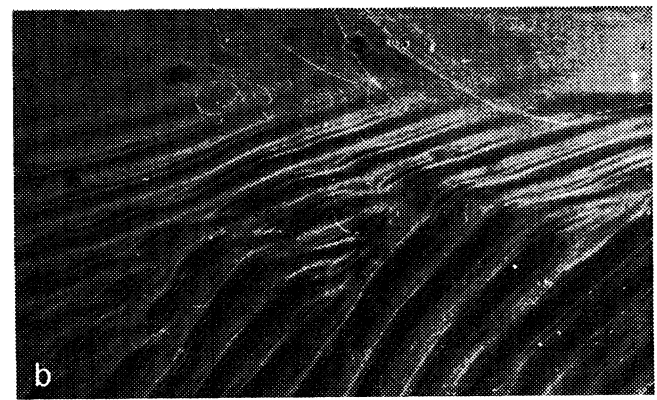
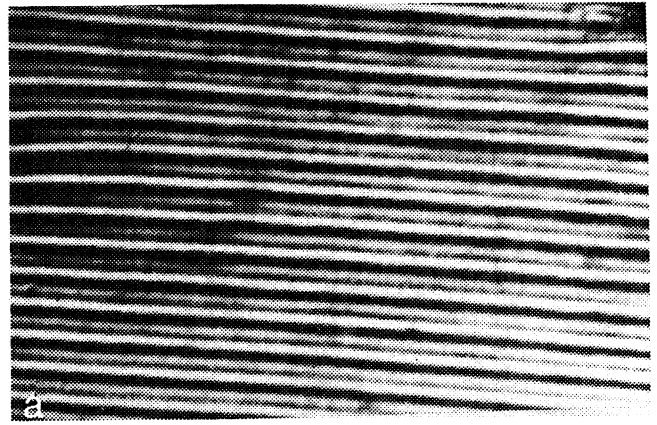


FIG. 2. Optical pattern of the distortion of the director field on different sections of the layer at and above the instability threshold: a) Striped structure at the instability threshold; $d=60 \mu\text{m}$, $f=5 \text{ Hz}$, $\psi_0=90^\circ$; b) coexistence of striped structures with different wave vectors q ; $d=60 \mu\text{m}$, $f=20 \text{ Hz}$, $\psi_0=90^\circ$; c) incommensurate structures above threshold ($\xi/\xi_{0 \min} \sim 1.4$); $d=60 \mu\text{m}$, $f=20 \text{ Hz}$, $\psi_0=90^\circ$.

normalized equal 2.6, 3, 4, and 4.6 (10^5 m^{-1}) for frequencies 2, 5, 15, and 20 Hz, respectively.

The characteristics described above are observed in the entire experimental frequency range for samples of thickness

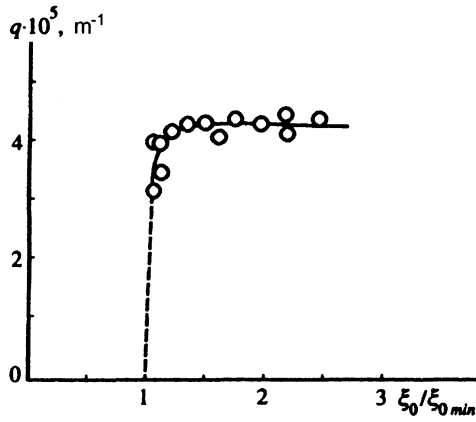


FIG. 3. Wave number q of the distortion of the director field versus the level of the action; $d=35 \mu\text{m}$, $f=20 \text{ Hz}$, $\psi_0=90^\circ$.

10–150 μm . The results of these observations are summarized in Fig. 5. Here, the values of q which are produced in 35–150 μm thick layers with ψ_0 in the range $0-90^\circ$ for oscillation frequencies 6.28–125.6 s^{-1} (symbols 1–18) are displayed together with the data of Ref. 7 (inset) on the periodicity of a striped structure under the conditions $\psi_0=0$ and $d=10 \mu\text{m}$ with oscillation frequencies of 62.8–628 s^{-1} . The symbols are explained in the caption. The values of q and ω are normalized here to the parameter $p = \pi/d$. This makes it easier to compare the experimental data with the plots which follow from the theoretical model,⁸ which in the range of values $\psi_0 \rightarrow 90^\circ$ predicts an analytic dependence of the form $q/p \propto (\omega/p^2)^{1/3}$. Analysis of the experimental values of q/p which are presented in Fig. 5 shows that as the oscillation frequency of the flow decreases with $p = \text{const}$, the wave number of the structure decreases and passes into the range of values $q \leq p$, the changes being most pronounced for values of ψ_0 close to 90° and less noticeable for $\psi_0 < 45^\circ$.

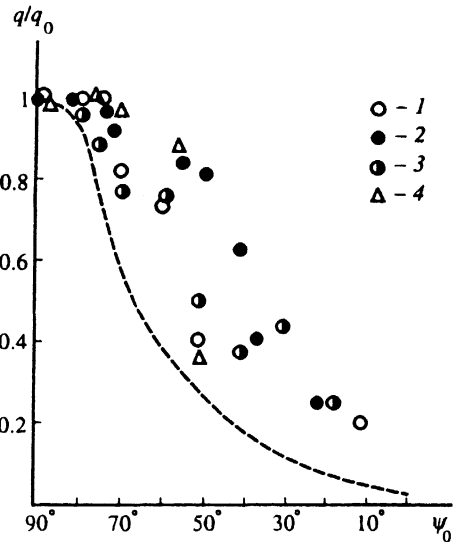


FIG. 4. Effect of the angle on the wave numbers of the distortion for oscillation frequencies of 2, 5, 15, and 20 Hz (symbols 1–4); $d=35 \mu\text{m}$; q_0 is the value of the wave number for $\psi_0=90^\circ$ at the indicated frequencies. The dashed curve represents the theoretical function $q(\psi)/q_0$ with $\omega/p^2=2.8 \cdot 10^{-3} \text{ cm}^2/\text{s}$.

Let us now examine the main phenomena that characterize the magnitude of the action at the threshold of instability. The family of curves in Fig. 6 illustrates the effect of the angle ψ_0 on the threshold gradient for NLC layers 30, 60, and 90 μm thick, respectively, at frequency $f=2 \text{ Hz}$. It follows from these data that as the angle ψ_0 changes, the largest changes in the threshold gradient occur in thin NLC layers. The experimental data presented in Fig. 7 show that an instability whose threshold gradient exhibits the following features develops in the experimental frequency range: It increases linearly with the oscillation frequency and decreases as ψ_0 increases. Here, the symbols 1–7 show the values of $S_{0 \text{ min}}$ for 30–90 μm thick layers and the following values of

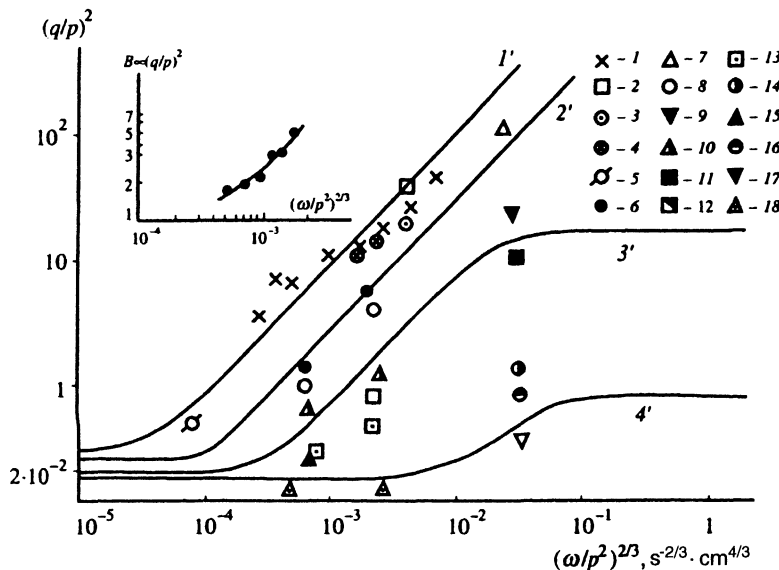


FIG. 5. Comparison of the experimental and theoretical threshold characteristics. a) q versus frequency for $\psi_0=90^\circ$, 67.5° , 45° , and 8.6° (theoretical curves 1'–4'); experimental data for ψ_0 and d : 1– 90° , $d=30 \mu\text{m}$, 2– 90° , $35 \mu\text{m}$, 3– 90° , $50 \mu\text{m}$, 4– 90° , $80 \mu\text{m}$, 5– 80° , $10 \mu\text{m}$, 6– 70° , $35 \mu\text{m}$, 7– 70° , $150 \mu\text{m}$, 8– 60° , $35 \mu\text{m}$, 9– 57° , $150 \mu\text{m}$, 10– 50° , $35 \mu\text{m}$, 11– 45° , $150 \mu\text{m}$, 12– 40° , $35 \mu\text{m}$, 13– 30° , $35 \mu\text{m}$, 14– 22.5° , $150 \mu\text{m}$, 15– 20° , $35 \mu\text{m}$, 16– 11.2° , $150 \mu\text{m}$, 17– 0° , $150 \mu\text{m}$, 18– 0° , $35 \mu\text{m}$. Inset—data from Ref. 7.

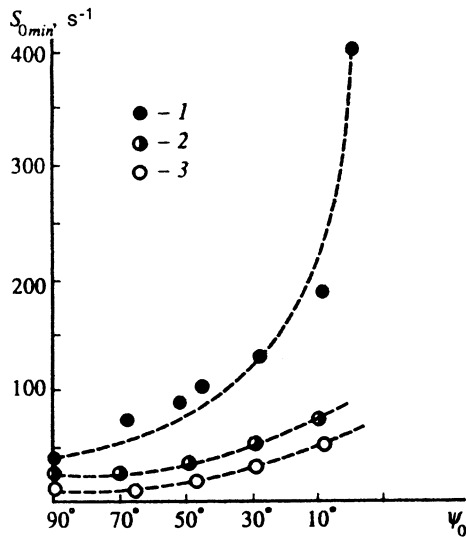


FIG. 6. Relation between the threshold gradient $S_{0\min}$ and the angle ψ_0 for 30, 60, and 90 μm thick NLC samples (symbols 1–3), $f=2$ Hz.

the angle ψ_0 : 90° (1), 70° (2 and 3), 50° (4 and 5), 35° (6), and 10° (7).

We now compare the experimental data on the behavior of the threshold characteristics with the theoretical model. The linearized system of equations, presented in Ref. 8, for the deflection angles θ_1 and ψ_0 of the director and the flow velocities V_x, V_y , and V_z describes in the present physical situation all characteristic features of the NLC for which the Leslie viscosity coefficients α_1, α_3 , and α_6 are small compared with the coefficients α_2 and α_4 . Analysis of this sys-

tem for the existence of periodic undamped solutions $\theta_1(t)$ and $\psi_1(t)$ leads to the following condition:⁸

$$S_0^2(q^2) = \{2b_1^2b_2^2 + a_1a_2\omega^2[b_1^2 + b_2^2 \pm (b_1^2 - b_2^2)]\} / c_1c_2b_1b_2, \quad (1)$$

where a_1, a_2, b_1, b_2, c_1 , and c_2 are coefficients which depend on ψ_0, α_i, K_i, p , and q (K_i are the Frank elastic constants). The corresponding expressions for them, which are not presented here because of their complexity, can be found in Ref. 8. The values of ψ_0 and ω for which this analysis is correct are determined by the following inequalities:

$$\frac{\pi^2 K_i \sin \psi_0}{\sqrt{\alpha_2 \alpha_3} d^2} < \omega \ll \frac{8 \pi^2 \sqrt{\alpha_2 \alpha_3}}{\rho d^2},$$

$$|\psi_0|, |\psi_0 - \pi| < \sqrt{|\alpha_3 / \alpha_2|}. \quad (2)$$

The threshold characteristics $S_{0\min}$ and q of the instability are found the same way by minimizing the functional dependence $S_0(q)$. The results are displayed in graphical form in Figs. 5 and 7. These are plots of the wave number q of the striped structure at $S_0 = S_{0\min}$ and the threshold gradient $S_{0\min}$ versus the oscillation frequency in the range $10^{-2} - 10^2 \text{ s}^{-1}$ for $\psi_0 = 90^\circ, 67.5^\circ, 45^\circ$, and 8.6° (plots 1'–4'). The values of q/p in Fig. 5 refer to layers 30–150 μm thick, and the thresholds $S_{0\min}$ in Fig. 7 correspond to $d = 30$ and $100 \mu\text{m}$ (solid and dashed lines). It follows from the plots 1'–4' presented in Fig. 5 that, depending on the values of the angle ψ_0 , different instability modes can appear in an oscillatory plane Couette flow: a) Guyon–Pieranski instability with a wave vector \mathbf{q} that depends on the oscillation frequency of the flow and on the thickness of

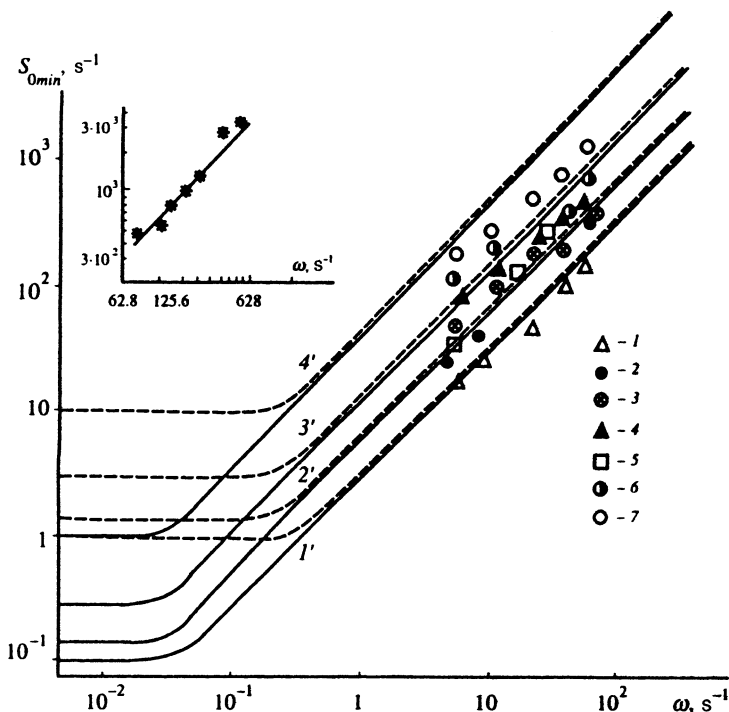


FIG. 7. Threshold gradient versus frequency for $\psi_0 = 90^\circ, 67.5^\circ, 45^\circ$, and 8.6° (theoretical curves 1'–4') for 90 and 30 μm thick samples (solid and dashed lines); experimental values of $S_{0\min}$: 1— $\psi_0 = 90^\circ, d = 90 \mu\text{m}$; 2— $70^\circ, 90 \mu\text{m}$; 3— $70^\circ, 30 \mu\text{m}$; 4— $50^\circ, 30 \mu\text{m}$; 5— $50^\circ, 90 \mu\text{m}$; 6— $35^\circ, 30 \mu\text{m}$; 7— $10^\circ, 30 \mu\text{m}$. Inset: $\psi_0 = 0^\circ, d = 10 \mu\text{m}$.

the layer and b) an instability whose wave vector is determined by the thickness of the layer. For values of ψ_0 in the range 90° – 67.5° the form of the function $q(\omega)$ does not change as the angle changes, i.e., the instability is seemingly not affected by the angle, and the values of q grow without bound as ω increases (plots 1' and 2'). For $\psi_0=46^\circ$ and 8.6° (plots 3' and 4') an instability mode with smaller wave numbers develops. Its characteristic feature is that as ω increases, the wave number q approaches a finite limit that depends on ψ_0 . According to the theory of Ref. 8, the critical angle separating the regions where different instability modes exist depends only on the viscosity coefficients of the NLC and equals

$$\psi_{0cr} \sim \tan^{-1} \sqrt{1 + 2\alpha_3 / \sqrt{\alpha_2 + \alpha_5}}. \quad (3)$$

For MBBA at 23°C $\psi_{0cr}=44.2^\circ$. The experimental results presented in Fig. 5 confirm the following results of the theory: For the striped structure arising under the conditions $\psi_0 > \psi_{0cr}$ ($\psi_0=90^\circ$, symbols 1–4; $\psi_0=80^\circ$, symbols 5) the values of q cluster near the theoretical curve 1', which represents the function $q(d, \omega, \psi)$ for $\psi_0=90^\circ$; the changes in the values of q for structures formed in the range of angles 70° – 57° (symbols 6–9) agree with the curve 2' corresponding to the angle $\psi_0=67.5^\circ$; the wave numbers of the structures arising in the situations $\psi_0 \approx \psi_{0cr}$ and $\psi_0 \leq 30^\circ$ (symbols 10–12 and 13–18) lie near the theoretical curves 3' and 4', which correspond to $\psi_0=45^\circ$ and 8.6° .

The theoretically predicted changes in the threshold gradient of the instability in the range of values of d , ω , and ψ_0 studied also agree with the experimental data (Fig. 7). The values of $S_{0\min}$ for structures arising in the range of angles $\psi_0 > \psi_{0cr}$ ($\psi_0=90^\circ$, $d=90\ \mu\text{m}$, symbols 1; $\psi_0=70^\circ$, $d=90\ \mu\text{m}$ and $d=30\ \mu\text{m}$, symbols 2 and 3) cluster near the curves 1' and 2', which illustrate the form of the function $S_{0\min}(\omega)$ for $\psi_0=90^\circ$ and 67.5° . The symbols 4 ($\psi_0=50^\circ$, $d=30\ \mu\text{m}$), 5 ($\psi_0=50^\circ$, $d=90\ \mu\text{m}$), and 6 ($\psi_0=35^\circ$, $d=30\ \mu\text{m}$) represent the thresholds at angles close to the critical angle: The corresponding points lie on the curve 3' corresponding to the case $\psi_0=45^\circ$. The values of $S_{0\min}$ for the modulated structure arising at $\psi_0=10^\circ$ (symbols 7, $d=30\ \mu\text{m}$) are close to the theoretical curve 4' ($\psi_0=8.6^\circ$).

It follows from the condition (2) that for a NLC of the type MBBA in the region $[0, 90^\circ]$ angles $\psi_0 < 6.3^\circ$ are not studied (at temperature 21°C). For this reason, theoretical plots representing the threshold characteristics of the instability that develops in the case when the vectors \mathbf{n}_0 and \mathbf{V} are parallel to one another ($\psi_0=0$) are not displayed in Figs. 5 and 7. As we have already mentioned, this situation was studied in Ref. 7 for a $10\ \mu\text{m}$ thick layer at frequencies in the range 20–100 Hz. These data on the frequency dependences of the parameter $B \propto (q/p)^2$ and the threshold $S_{0\min}$ at a temperature of 19°C for the liquid crystal ZLI-518 are displayed in the insets in Figs. 5 and 7. These results agree qualitatively with the theoretical instability threshold characteristics for MBBA, which are represented by the plots 4' ($\psi_0=8.6^\circ$).

Comparing with the theoretical results (see the dashed line in Fig. 4; this line corresponds to the ratio

$\omega/p^2=2.8 \cdot 10^{-3}\ \text{cm}^2/\text{s}$) the experimental data on the angular dependence of the wave numbers obtained for a striped structure (q/q_0) in the frequency range 2–20 Hz with a constant layer thickness ($d=35\ \mu\text{m}$) reveals the following anomalies: The experimental values of q/q_0 are shifted in the direction of lower values of ψ_0 , and as ψ_{0cr} is approached they decrease more slowly than predicted by the theory.

We now discuss the possible reasons for this anomaly. In the experimental arrangement the moving plate in the oscillatory system (bearing plate—NLC layer—cover plate) can undergo “parasitic” piston oscillations of the form

$$\xi_z(t) = \beta \varepsilon_{0y} \sin(\omega t + \varphi)$$

in the direction of the z axis. At low frequencies these oscillations give rise to a circular periodic flow of an incompressible nematic liquid with velocity

$$V_r(r, z, t) = \text{const} \cdot r(z^2 - zd) \sin(\omega t + \varphi) \quad (4)$$

in the direction of the open ends of the layer. Here, \mathbf{r} is the radius vector, φ is the phase shift between the piston and shear (main) oscillations, and $\xi_{0z} = \beta \xi_{0y}$ is the amplitude of the piston oscillations. Under the combined action of shear (main) and piston (parasitic) oscillations on the NLC a non-uniform oscillatory flow—the result of the superposition of Couette and Poiseuille flow—with a velocity distribution different from that in a planar Couette flow is established in the layer. The following effects can be expected to appear in this situation:

a) The distinguished direction of the relative orientation of the vectors \mathbf{n} and \mathbf{V}_s “vanishes” and the angle ψ_0 can take on a number of possible values (right up to 90°). This leads to the appearance of structures with larger wave numbers on separate sections of the layer than the wave numbers that follow from the values of ψ_0 , d , and ω prescribed in the experiment in the case of planar Couette flow; $\mathbf{V}_s(y, z, t)$ is the velocity vector of the nonuniform total flow.

b) The orientation of the wave vector \mathbf{q} changes: It can tilt away from the x axis and assume a position determined by the direction of the nonuniform flow for the given values of ω and d . The photomicrograph displayed in Fig. 2b illustrates this effect.

It is obvious that under the influence of these factors the true value of the angle ψ_0 under real conditions will differ from the initially prescribed arrangement of the vectors \mathbf{n}_0 and \mathbf{V}_{0y} , and it will be largely determined by the position of the observation zone in the xy plane. In the light of what has been said above, the shift, observed experimentally at a number of frequencies, of the plots of the function $q(\psi_0)/q_0$ in the direction of lower values of ψ_0 is completely natural (Fig. 6). As shown in Ref. 10, for an oscillatory system of the type considered here the coefficient $\beta = \xi_{0z}/\xi_{0x}$ characterizing the importance of the parasitic component depends on ω and d , and it can vary from 0.001 to 0.9 in the frequency range $1 - 10^4$ Hz. Therefore, in the situation under discussion, the effect of parasitic piston oscillations will be appreciable only at some frequencies. This effect can also exhibit a definite selectivity with respect to the position of the observation zone in the plane of the layer, since the flow

velocity depends on the coordinate r and assumes its largest value at the ends of the layer (see Eq. (4)). Indeed, the observations showed that near the ends of the layer, at some frequencies, even with a very small excess above the threshold displacement $\xi_{0y,\min}$, the striped one-dimensional structure transforms into a two-dimensional structure, and once again a one-dimensional structure exists in the zones adjacent to the center of the flow. The photomicrograph in Fig. 2c shows the pattern of the distortion in the zone near the edges of the layer for ξ_{0y} equal to, correspondingly, $1.4\xi_{0y,\min}$, i.e., above threshold; here, $d=60\ \mu\text{m}$, $f=3\ \text{Hz}$, and $\psi_0=\pi/2$. These incommensurate structures (system of dashes) are the result of an additional spatial modulation appearing in the initial striped structure when the amplitude of the parasitic oscillations reaches appreciable values, which apparently happens only above threshold. To check this supposition, we performed an experiment in which the additional exciter (of the piston oscillations) produced a periodic compression of the layer at the frequency of the main (shear) oscillations; this induced an oscillatory, circular Poiseuille flow. The conditions of this experiment were as follows: $d=15-60\ \mu\text{m}$, $f=4-15\ \text{Hz}$, and $\beta=0.01-0.1$. The observations showed that if the frequency of the main exciter equals the frequency of the secondary exciter, then incommensurate structures similar to those displayed in Fig. 2c appear for any of the above values of β ; this is a direct confirmation of the hypothesis.

4. CONCLUSIONS

As a result of the study of the instability of the planar structure of a NLC under acoustic-hydrodynamic action for arbitrary angles between the velocity vector \mathbf{V} of the oscillatory hydrodynamic flow and the director \mathbf{n}_0 , incommensurate structures and different types of striped structures were observed.

It follows from the analysis presented above that it is convenient to classify the characteristics of the striped structures with the aid of the ratio ψ_0/ψ_{0cr} : For $\psi_0/\psi_{0cr}<1$, there exists a range of frequencies where the period Λ of the structure does not depend on the oscillation frequency of the flow and is determined by the thickness of the NLC layer; if $\psi_0/\psi_{0cr}\geq 1$, then the period of the structure depends on the frequency and can be much smaller than the thickness d of the layer (these relations correspond to the classical behavior of the Guyon–Pieranski roll instability⁴ observed in the particular case $\psi_0/\psi_{0cr}\sim 2$ ($\psi_0=90^\circ$); the threshold gradient $S_{0\min}$ for arbitrary values of ψ_0/ψ_{0cr} depends on the frequency and increases linearly with ω . The threshold characteristics $S_{0\min}$ and Λ for the striped structure are described satisfactorily by a generalized theoretical model⁸ based on the standard Leslie–Ericksen–Parodi hydrodynamics. This shows that this approach can be used to describe the orientational phenomena initiated by acoustic-hydrodynamic action for arbitrary relative orientation of the vectors \mathbf{n}_0 and \mathbf{V} and oscillation frequencies satisfying the condition (2).

It also follows from what we have said above that the superposition of Couette and Poiseuille flows strongly affects the distortion of the director field \mathbf{n}_0 . At the stability threshold this influence is manifested as an anomalous displace-

ment of the plots of the functions $q(\psi_0)/q_0$ corresponding to some frequencies, and above threshold it results in the formation of incommensurate structures. It is interesting to note that the behavior of the striped structure above threshold was analyzed in Ref. 11 in application to the effect of an electric field (flexoelectric effect). In this case the mechanism by which the period of the flexostructure decreases as the field increases is dislocation production.

In the situation discussed here, the incommensurate structures are the result of a spatial modulation of the initial striped structure. The observations showed that at the initial stage of these transformations individual stripes are ruptured, so that the strips are seemingly separated into narrow zones by quite regular line segments of length $(1-10)\Lambda$; then, the relative arrangement of these zones changes in a disordered manner, i.e., line segments seem to move and bend randomly; after 2–3 s the initial ruptures vanish, but new ruptures appear in other stripes and the transition from regular stripes to stripes separated into zones is repeated. Ultimately, a balance, where the annihilation of some defects is accompanied by the appearance of other defects, is established in the NLC system, and in some regions of the layer the above-described transition leads to the formation of stripes in which the lines of rupture are separated by equal distances from one another and are arranged in a direction perpendicular to the flow velocity. As the oscillation amplitude increases, these regions grow and merge, so that ultimately the characteristic incommensurate structure shown in Fig. 2c is formed throughout the entire layer. The analysis of the defects appearing in a striped structure above threshold and their dynamics falls outside the scope of our work. This aspect of the problem was considered at the present stage of the investigations only in connection with the discussion of the hypothesis advanced as possible reasons for the transformation of the striped structures that are characteristic for Couette flow.

In closing, it should be noted that the investigations performed not only revealed new physical aspects in the classical problem of the instability of a NLC in oscillatory hydrodynamic flow, but they also made it possible to determine the combination of parameters d , ω , and ψ_0 for which regular striped structures can be used as acoustically controlled phase gratings.

This work was performed with the financial support of the International Science Foundation Grant No. J7D100.

¹The striped structure consists of a grating with periodic variation of the index of refraction. For this reason, when light with wavelength λ_0 and polarization vector $\mathbf{E} \parallel \mathbf{n}_0$ passes through it, a diffraction pattern with a distribution of maxima and minima along a line parallel to the x axis appears on the screen.

¹A. P. Kapustin and O. A. Kapustina, *Acoustics of Liquid Crystals* [in Russian], Nauka, Moscow, 1986.

²S. A. Pikin, *Structural Transformations in Liquid Crystals* [in Russian], Nauka, Moscow, 1981.

³D. I. Anikeev, O. A. Kapustina, and V. N. Lupanov, *Zh. Éksp. Teor. Fiz.* **100**, 197 (1991) [*Sov. Phys. JETP* **73**, 109 (1991)].

⁴P. Pieranski and E. Guyon, *J. de Phys.* **36**, 203 (1975).

⁵E. Dubois-Violette, E. Guyon, I. Janossy *et al.*, *J. de Mécanique* **16**, 733 (1977).

⁶E. Guyon and P. Pieranski, *Phys. Rev.* **9**, 404 (1974).

⁷M. G. Clark, F. C. Saunders, I. A. Shanks, and F. M. Lelsie, *Mol. Crys. Liq. Crys.* **70**, 195 (1981).

⁸V. N. Reshetov, *Akustich. Zh.* **31**, 639 (1985) [*Sov. Phys. Acoustics* **31**(5), 383 (1985)].

⁹P. Manneville, *J. de Phys.* **39**, 911 (1978).

¹⁰O. A. Kapustina, E. N. Kozhevnikov, and G. N. Yakovenko, *Zh. Éksp. Teor. Fiz.* **87**, 849 (1984) [*Sov. Phys. JETP* **60**, 483 (1984)].

¹¹E. M. Terent'ev and S. A. Pikin, *Zh. Éksp. Teor. Fiz.* **83**, 1038 (1982) [*Sov. Phys. JETP* **56**, 587 (1982)].

Translated by M. E. Alferieff